Relativistic pseudopotentials for transition metals. I. Construction and application to atoms

1990 J. Phys.: Condens. Matter 2 7101

(http://iopscience.iop.org/0953-8984/2/34/004)

J. Phys.: Condens. Matter **2** (1990) 7101–7114. Printed in the UK

Relativistic pseudopotentials for transition metals: I. Construction and application to atoms

V Yu Milman†‖, V N Antonov‡¶ and V V Nemoshkalenko§

† University of Cambridge, Cavendish Laboratory, TCM Group, Cambridge CB3 0HE, UK

‡ Max-Planck Institute für Festkörperforschung, Postfach 800665, 7000 Stuttgart 80, Federal Republic of Germany

§ Institute of Metal Physics of the Ukrainian Academy of Sciences, 36 Vernadsky Street, Kiev 252142, USSR

Received 9 January 1990, in final form 4 June 1990

Abstract. A technique of *ab initio* fully relativistic pseudopotential construction has been developed and used to construct pseudopotentials (PP) for all transition metals. Systematic trends in the Periodic table have been studied. It was shown that the correct evaluation of relativistic effects in the Dirac approximation could be of greater importance for transition metals than for simple metals due to specific features of the valence electron density distribution. Test calculations for a variety of atoms and atomic configurations indicated good transferability of our PPs. The influence of ionic radii and of the particular choice of exchange–correlation potential on the PP obtained was studied. LDA relativistic results were found to be qualitatively accurate in atomic spectra studies.

1. Introduction

Intensive development of *ab initio* pseudopotential (PP) calculations during the last decade [1–3] have shown the necessity of using an ionic non-local PP. This approach has enabled solid state physicists, using band structure studies, to make *ab initio* predictions of such properties as lattice dynamics [1, 2] and the electron–phonon interaction both at ambient conditions [3] and under substantial pressure [4]. Techniques have been developed for *ab initio* determinations of structural phase transition temperatures [5], and phonon–phonon coupling has been studied to provide an explanation of high-temperature phase stability [6]. *Ab initio* density-functional calculations with the use of PPs have been performed not only for elemental solids but also for compounds and alloys of metals [7] and of semiconductors [8] where the heat of formation and other lattice properties have been studied.

One of the main requirements which an *ab initio* PP designed for solid state studies must meet is the correct description of ionic core scattering properties. It is just this feature which enables transferability of the PP, i.e. the potential obtained describes exactly the electron scattering process for different atomic environments. In this intro-

‖ On leave from the Institute of Metal Physics, Kiev 252142, USSR.

¶ Permanent address: Institute of Metal Physics, Kiev 252142, USSR.

0953-8984/90/347101 + 14 $03.50

ductory section different methods of *ab initio* PP construction will be reviewed briefly, and in the following sections a fully relativistic technique will be suggested.

An *ab initio* PP is usually calculated using density-functional theory (DFT) for free atoms or ions [9–12]. The idea of the introduction of an effective PP instead of the full potential for the nucleus has already been used successfully in atomic and molecular physics. A comprehensive review of non-relativistic atomic calculations was given in [13], where the method of taking into account relativistic effects in the Dirac–Hartree–Fock approach was also proposed.

We wish only to comment here on the term 'norm-conserving PP' since details of the non-relativistic procedure have been given elsewhere [9–12]. Usually a non-relativistic DFT PP $V_l(r)$ is obtained from an inversion of the Schrödinger equation for a certain pseudo wavefunction $\varphi_l(r)$, initially chosen as a linear combination of true wavefunctions ψ_l giving rise to a singular PP [9]. In this case φ_l and ψ_l can be made identical outside the core only if the norm of the pseudo wavefunction is not kept, leading to the orthogonality hole problem. A norm-conserving PP enables this problem to be avoided by exactly equating the normalised φ and ψ outside the core. Different methods have been suggested for this purpose resulting in non-singular [10, 11] as well as in singular PPs [12] with the same behaviour at $r \to 0$ as the PP from [9]. Singular PPs are suitable for structural mapping of binary compounds [14–16] with little use elsewhere, so we shall only treat non-singular PPs here.

All potentials mentioned above have been used with sufficient success when computing crystal properties in the framework of the local density approximation (LDA) (see e.g. [17]). Surprisingly, a LDA PP appeared even to give the same electron spectrum as the full atomic potential in an unrestricted HF calculation [18].

The idea of a relativistic PP approach suitable for heavy elements was first introduced in atomic Dirac–Hartree–Fock calculations [13, 19]. The relativistic LDA version of the PP approach was suggested by Kleinman [20] and realised numerically two years later in a classic work by Bachelet *et al* [21]. Relativistic coupled equations for the valence electrons were transformed into the non-relativistic Schrödinger equation; thus all relativistic effects were contained in a non-relativistic PP similarly to the results of [13]. Another approach chosen in [19] led to a fully relativistic spin-polarised approach with the PP represented by a 4×4 matrix which seems to be inappropriate for LDA solid state calculations.

A modified scalar relativistic treatment proposed in [20, 21] and widely exploited later was based initially on Dirac's coupled pair equations for major and minor wavefunction components $g(r)$ and $f(r)$

$$\begin{cases} G' + \kappa G/r = (2\alpha^{-2} + \varepsilon - V(r))\alpha F \\ F' - \kappa F/r = (V - \varepsilon)\alpha G \end{cases} \tag{1.1}$$

where $G(r) = rg(r)$, $F(r) = rf(r)$ and $\kappa = (l - j)(2j + 1)$ is a relativistic quantum number. Atomic units with $\hbar = m = e = 1$ and $\alpha = c^{-1} = 137.037^{-1}$ are used here and throughout the paper unless otherwise stated. Neglecting the $(\varepsilon - V)$ term in the first equation of (1.1) one may easily obtain a Schrödinger-type equation for the major component only, which is then inverted as in the non-relativistic case [10]†.

† Usually the PP obtained in this approach is further used in the fully non-relativistic (or scalar relativistic) band structure calculation. The recent article by Elsässer *et al* [42] serves as an example of such an approach, where the authors claimed to study relativistic effects but even the huge spin–orbit splitting for 5d metals was not taken into account.

At this point several questions inevitably arise. First of all, this approach is not well grounded for the core region, $r < r_c$, where the d component of the PP is quite substantial, reaching e.g. hundreds of Rydbergs for 3d elements (see [22] or the present results, section 4). The correctness of the spin–orbit splitting treatment in terms of weighted sums and differences of the PP, corresponding to different values of the total angular-momentum quantum number, j, and to the same value of the angular quantum number, l, is also doubtful.

Taking this into account we aimed to develop a method of band structure and total energy calculations in Dirac's formalism. The first step described in this paper is concerned with the calculation of a relativistic *ab initio* PP. This procedure is presented in section 2 while the results of atomic test calculations for all transition metals are given in section 3. Section 4 is concerned with trends in PP characteristics observed in the Periodic table.

2. Construction of the relativistic PP

We recall that, by correctly taking into account relativistic effects, one may expect to gain accuracy mainly in the study of heavy transition metals where the PP in the core region is not small [22] and the wavefunction for d states is highly localised near the nucleus.

The procedure suggested here includes several steps:

(i) As in [21] we solve Dirac's equation (1.1) for a chosen atomic reference configuration, thus obtaining valence energies ε_κ, radial wave-functions F_κ and G_κ, and a total self-consistent atomic potential V_{at}. The atomic problem was considered within the LDA, V_{xc} was chosen to be in the Ceperley–Alder form [23] as parametrised by Perdew and Zunger [24]. Other LDA expressions [25, 26] for V_{xc} were also used for comparison. Following [21] we account for relativistic effects (transverse photon–electron interaction, retardation of the Coulomb electron interaction) in the form proposed by Macdonald and Vosko [27]. This leads to multiplication of the exchange energy ε_x and potential V_x by additional factors f_ε and f_V, respectively

$$\begin{aligned} f_\varepsilon(\rho) &= 1 - 1.5\{(1+\beta^2)^{1/2}/\beta - \ln[\beta + (1+\beta^2)^{1/2}]/\beta^2\}^2 \\ f_V(\rho) &= -0.5 + 1.5\ln[\beta + (1+\beta^2)^{1/2}]/\beta(1+\beta^2)^{1/2} \end{aligned} \tag{2.1}$$

where $\beta = 0.0140/r_s = v_F(\rho)/c$ is the parameter which measures the Fermi velocity, and $r_s = (3/4\pi\rho)^{1/3}$. Relativistic corrections are important in regions with large β, i.e. a high density, ρ. Here the usual LDA definitions for $V_{xc}(\rho(r))$ and for $\rho(r)$ in terms of $G(r)$ and $F(r)$ were used [17]. (Note that equations for f_ε and f_V, namely (3.4) from [27] and (2.8) from [21], contain misprints.)

Reference atomic configurations for the transition element series were chosen according to [21]. PPs acting on s and d states were determined using free atom configurations, while p and f components were obtained from single- and double-ionised configurations, respectively. Both spin–orbit components were always occupied according to their multiplicities $(2j + 1)$ giving the reference configuration

$$ns^{3/4}_{1/2}np^{1/12}_{1/2}np^{1/6}_{3/2}(n-1)d^{0.4(Z_v-2)}_{3/2}(n-1)d^{0.6(Z_v-2)}_{5/2}$$

for the p potential, where Z_v is the number of valence electrons, and for the f potential we obtain correspondingly the reference configuration

$$ns^{3/4}_{1/2}(n-1)d^{0.4(Z_v-3)}_{3/2}(n-1)d^{0.6(Z_v-3)}_{5/2}(n-1)f^{3/28}_{5/2}(n-1)f^{1/7}_{7/2}.$$

(ii) We construct an intermediate PP $V_\kappa^{(1)}$ regular in the $r \to 0$ limit by cutting off the short-range part of the atomic potential, V_{at}

$$V_\kappa^{(1)} = V_{at}(1 - f_c(r/r_{c\kappa})) + C_\kappa f_c(r/r_{c\kappa}). \tag{2.2}$$

A cut-off function $f_c(x) = \exp(-x^\lambda)$ with $\lambda = 3.5$ was chosen as in [21], while the constant C_κ was adjusted so that equations (1.1) with the $V_\kappa^{(1)}$ potential had the eigenvalue equal to the atomic one ε_κ, and the corresponding radial function $G_\kappa^{(1)}(r)$ was nodeless. We have $V_\kappa^{(1)} \to V_{at}$ beyond the core region, so for $r > r_{c\kappa}$

$$\gamma_\kappa G_\kappa^{(1)}(r) \to G_\kappa^{at}(r) \qquad \gamma_\kappa F_\kappa^{(1)}(r) \to F_\kappa^{at}(r) \qquad r \to \infty \tag{2.3}$$

since intermediate and atomic wavefunctions satisfy the same differential equation and boundary conditions for $r > r_{c\kappa}$. Cut-off radii were obtained as $r_{c\kappa} = r_\kappa^{max}/K_l$, where r_κ^{max} was the position of the outermost peak in $G_\kappa^{at}(r)$. Values of the K_l parameters were slightly increased compared with [21] being equal to 1.9, 1.7 and 3.0 for 3d elements, 1.9, 1.7 and 1.7 for 4d elements, and 1.7, 1.7, 1.6 and 3.0 for 5d elements, where the f component of the PP was also calculated. This decrease of $r_{c\kappa}$ leads to more compact PPS which may be preferable in real-space band structure calculations [28, 29]. Potential matrix elements would be essentially simplified in the approach mentioned if the non-local part of the PP (i.e. $V_\kappa^i + Z_v/r$) centred on different atoms did not overlap [29].

(iii) We modify the PP in the core region in order to obtain pseudo wavefunctions G_κ^{ps}, F_κ^{ps} coinciding with atomic ones for $r > r_{c\kappa}$. In this way the norm-conserving condition is satisfied, resulting in a good PP transferability. At this step we transform the major component $G_\kappa^{(1)}$ in the following way

$$G_\kappa^{ps}(r) = \gamma_\kappa(G_\kappa^{(1)}(r) + \delta_\kappa r^{l+1} f_c(r/r_{c\kappa})). \tag{2.4}$$

In the $r \to \infty$ limit we obtain $G_\kappa^{ps} \to \gamma_\kappa G_\kappa^{(1)} \to G_\kappa^{at}$ in view of (2.3), while in the $r \to 0$ limit the asymptotic behaviour $G_\kappa(r) \sim r^{l+1}$ is retained. Using the modified major component (2.4) we obtain the minor one, F_κ^{ps}, by a numerical integration of the following equation

$$\begin{aligned} dF_\kappa^{ps}/dr = {} & \kappa F_\kappa^{ps}/r + (G_\kappa^{ps}/F_\kappa^{ps})\{2\alpha^{-1}(F_\kappa^{ps} - \gamma_\kappa F_\kappa^{(1)}) + \gamma_\kappa(\varepsilon_\kappa + V_\kappa^{(1)})\alpha F_\kappa^{(1)} \\ & - \gamma_\kappa \delta_\kappa r^l f_c(r/r_{c\kappa})\,[l + 1 + \kappa - \lambda(r/r_{c\kappa})^\lambda]\} \end{aligned} \tag{2.5}$$

where the particular shape of $f_c(x)$ has already been taken into account. The value of δ_l entering (2.4) and (2.5) is determined from the normalisation condition:

$$\int [(G_\kappa^{ps}(r))^2 + (F_\kappa^{ps}(r))^2]\,dr = 1. \tag{2.6}$$

Usually the correction introduced at this step is small since $|\gamma_\kappa^2 - 1|$ is of the order of 10^{-2} for s states and of 10^{-3} for all other states. Assuming $\gamma_\kappa = 1$ we see that the solution of (2.4)–(2.6) is simply $F_\kappa^{ps} = F_\kappa^{(1)}$, $G_\kappa^{ps} = G_\kappa^{(1)}$, and $\delta_\kappa = 0$.

(iv) The screened ionic PP $V_\kappa^{(2)}(r)$ is found by inverting the second equation of (1.1) taking into account (2.6):

$$\begin{aligned} V_\kappa^{(2)}(r) = {} & (2\alpha^{-2} - \varepsilon_\kappa)(1 - \gamma_\kappa F_\kappa^{(1)}/F_\kappa^{ps}) + V_\kappa^{(1)}\gamma_\kappa F_\kappa^{(1)}/F_\kappa^{ps} \\ & - \gamma_\kappa \delta_\kappa r^l f(r/r_{c\kappa})[l + 1 + \kappa - \lambda(r/r_{c\kappa})^\lambda]/F_\kappa^{ps}. \end{aligned} \tag{2.7}$$

From (2.7) it may be seen that outside the core region $V_\kappa^{(2)} \to V_\kappa^{(1)} \to V^{at}(r)$. If one neglects corrections made at the third step one would obtain simply $V_\kappa^{(2)} \equiv V_\kappa^{(1)}$ in view of $\gamma_\kappa = 1$.

(v) Finally, we obtain an unscreened ionic PP V_κ^i following (2.8) where the pseudo density ρ_{ps} constructed according to (2.9) is used

$$V_\kappa^i(r) = V_\kappa^{(2)}(r) - \int \rho_{ps}(r')/|r - r'|\, dr' - V_{xc}(\rho_{ps}) \tag{2.8}$$

$$\rho_{ps}(r) = \sum_\kappa Q_\kappa[(G_\kappa^{ps}(r)) + (F_\kappa^{ps}(r))^2]. \tag{2.9}$$

A non-linear potential [30, 31] may be constructed in this approach by using $V_{xc}(\rho_c + \rho_{ps})$ instead of $V_{xc}(\rho_{ps})$ in (2.8), where ρ_c is the electron density of core states. Application of non-linear PPs in band structure calculations was discussed in detail in [32] where a term $V_{xc}(\rho_c)$ was also added to (2.8) revealing the logical connection with the problem of exchange–correlation non-linearity. Note that the non-linear PP for tungsten computed in [32] converges to $-Z_v/r$ asymptotically only for $r > 5$ while the usual approach provides convergence at least for $r > 3$.

Subsequent modifications [33, 34] of the conventional procedure [21] may also be useful in the fully relativistic approach. These innovations were concerned with the cutoff function $f_c(x)$. In [33] it was shown that by choosing different $r_{c\kappa}$ in equations (2.2) and (2.4) one may obtain PPs with bound states corresponding to valence electrons and to outer-core ones as well. Such PPs appear to be more short-ranged than usual ones, and may be useful in real-space calculations [28, 29] for e.g. 5d metals, where 5p outer-core states may be treated as valence states. A similar modification of the cutoff function was applied in [34] which was aimed to obtain the PP rapidly decreasing in reciprocal space and applicable in momentum-space calculations [35]. In the present work the modifications mentioned above were not applied.

3. Transferability of PPs

A relativistic norm-conserving PP for tungsten is given in figure 1 as a representative example, and the corresponding valence wavefunctions are shown in figure 2. The latter figure clearly shows the reason for success of the usual transformation of Dirac's equations (1.1) to the Schrödinger-type one [20, 21].

This transformation is based on the fact that the minor component F_κ^{at} is significant only at $r < r_{c\kappa}$ where relativistic effects are important. Whilst constructing ionic PPs one replaces F_κ^{at} with a smooth function $F_\kappa^{ps}(r)$ which is substantially smaller than F_κ^{at} at $r < r_{c\kappa}$. Since the pseudo wavefunction coincides with the true atomic one outside the core region we have $F_\kappa^{ps} \ll G_\kappa^{ps}$ for $r > r_{c\kappa}$, so the transition from an atomic problem to a pseudoatomic one does diminish the relative contribution of the minor component to the electron density.

Figure 2 illustrates the influence of the presence of a highly space-localised d electron valence shell on the accuracy of the common procedure connected with neglecting the minor wavefunction component. Due to the significant difference between the $r_{c\kappa}$-values for the s, p and d states we obtain a considerable contribution from F_κ^{ps} to the pseudo-atomic density in the intermediate region, $r_{cd} < r < r_{cs}$. An analysis of figures 1 and 2

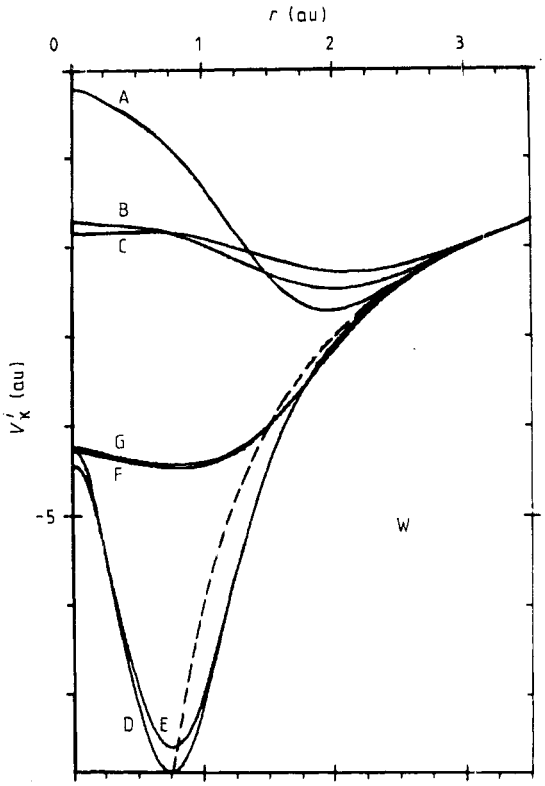

Figure 1. Norm-conserving relativistic PP for tungsten. A, $s_{1/2}$; B, $p_{1/2}$, C, $p_{3/2}$; D, $d_{3/2}$; E, $d_{5/2}$; F, $f_{5/2}$; G, $f_{7/2}$. The asymptotic $-Z_v/r$ is shown by the broken curve.

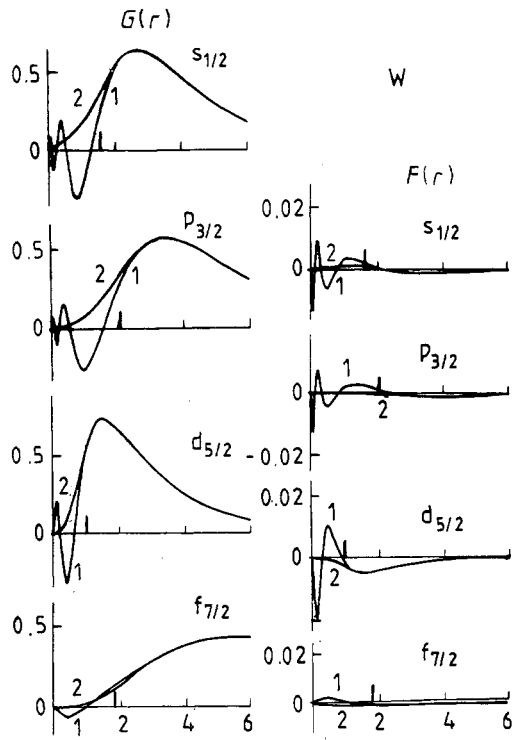

Figure 2. Valence wavefunctions for tungsten. Only $j = l + 1/2$ components are shown. Atomic functions G_κ^{at}; F_κ^{at} are marked as 1, pseudo wavefunction G_κ^{ps}, f_κ^{ps} are marked as 2. Vertical bars correspond to cutoff radii $r_{c\kappa}$.

shows that in this region the PP magnitude varies from 10 to 100 au for different elements, and so it is not negligible in comparison with α^{-2} in (1.1).

Let us consider now the problem of PP transferability which may be reformulated [10–12] in terms of a PP energy dependence. Results of atomic test calculations for tungsten are presented in table 1, and the same accuracy was obtained for 3d and 4d elements. The overall accuracy in the one-electron energies with respect to the all-electron calculation is better than 0.2% for occupied states irrespective of excitation energy E_{ex} for the configuration considered. Unoccupied states which were not included in the self-consistency procedure are described with slightly less accuracy, an error amounting in some cases to 1%. Note that the pseudoatomic self-consistent calculation is an order of magnitude faster than a similar all-electron study. The accuracy of the E_{ex} computation appeared to be even better than that of ε_κ being equal to nearly 0.1%.

Thus we have shown that the pseudoatomic calculation of the valence atomic states reproduces the LDA all-electron results accurately but with a substantially smaller computational effort. Therefore, we tried to study the applicability of the relativistic LDA to the electronic structure calculation of the transition series atoms using our PP generated with the above set of K_l values and with V_{xc} from [23, 24]. Excitation energies E_{ex} are given in table 2 for a number of configurations of free atoms and ions. Our data are compared with the experimental values and with the results of non-relativistic Hartree–Fock (HF) calculations [37]. Energies, quoted from [37] and obtained by the Cowan–Griffin (CG) method [38] (which approximately takes into account relativistic effects in the framework of the HF formalism), are also given in this table.

Table 1. Results of test atomic calculations for tungsten. ε_κ represents one-electron energies, E_{ex} is the excitation energy for the configuration considered. All-electron data are given in the upper row while deviations of pseudoatomic values are given in the lower row. The V_{xc} from [36] was used. All energies are in eV.

	ε_κ							
Configuration	$s_{1/2}$	$p_{1/2}$	$p_{3/2}$	$d_{3/2}$	$d_{5/2}$	$f_{5/2}$	$f_{7/2}$	E_{ex}
$d^4_{3/2}s^2_{1/2}$	4.835	1.037	0.627	3.727	3.025	—	—	0.000
	0.010	0.012	0.004	0.006	0.006	—	—	0.000
$d^4_{3/2}d^1_{5/2}s^1_{1/2}$	4.384	0.852	0.509	2.691	2.052	—	—	1.902
	−0.002	−0.003	−0.011	0.002	0.000	—	—	0.008
$d^4_{3/2}d^1_{5/2}p^1_{1/2}$	5.284	1.510	1.093	3.857	3.192	—	—	5.747
	0.001	−0.001	−0.010	0.001	0.000	—	—	0.014
$d^4_{3/2}s^1_{1/2}$	11.306	6.644	5.889	10.914	10.162	0.915	0.915	8.972
	0.014	0.014	0.007	0.014	0.015	0.000	0.000	0.014
$d^4_{3/2}d^1_{5/2}$	10.540	6.129	5.450	9.452	8.759	0.911	0.911	10.202
	−0.006	−0.012	−0.027	0.014	0.011	0.000	0.000	0.008
$d^4_{3/2}p^1_{1/2}$	12.050	7.262	6.468	11.955	11.182	0.995	0.995	12.656
	0.004	0.015	0.010	−0.009	−0.006	0.001	0.001	0.014
$d^4_{3/2}f^1_{5/2}$	15.045	9.766	8.782	15.593	14.785	2.043	2.042	19.548
	0.008	0.017	0.012	0.019	0.022	0.000	0.000	0.027
$d^4_{3/2}$	18.419	12.992	11.925	19.043	18.232	3.966	3.964	24.794
	0.009	0.018	0.011	0.022	0.025	0.002	0.002	0.029

Table 2. Excitation energies for atoms of transition elements. NHF: non-relativistic Hartree–Fock results [37]; HFR: results from [37] obtained by the Cowan–Griffin method [38]; PP: present results; EXP: experimental data from [37, 39].

		NHF	HFR	PP	EXP		NHF	HFR	PP	EXP
s^2d	Sc	0.00	0.00	0.00	0.00	Y	0.00	0.00	0.00	0.00
sd^2		1.00	1.12	1.57	1.43		0.42	0.75	1.67	1.36
d^3		4.47	4.65	4.03	4.19		2.73	3.32	3.71	3.63
sd	Sc^+	5.20	5.22	7.04	6.56	Y^+	4.72	4.81	6.77	6.64
d^2		6.14	6.32	7.64	7.16		5.48	6.02	7.70	7.53
s^2d^2	Ti	0.00	0.00	0.00	0.00	Zr	0.00	0.00	0.00	0.00
sd^3		0.54	0.68	1.06	0.81		−0.40	−0.01	1.10	0.59
d^4		4.26	4.48	3.35	3.35		1.71	2.44	2.83	2.66
sd^2	Ti^+	5.51	5.55	7.51	6.84	Zr^+	5.05	5.18	7.29	6.95
d^3		5.96	6.17	7.59	6.94		4.99	5.65	7.62	7.27
s^2d^3	V	0.00	0.00	0.00	0.00	Nb	0.00	0.00	0.00	0.00
sd^4		0.12	0.29	0.53	0.25		−1.24	−0.80	0.47	−0.18
d^5		3.27	3.55	2.63	2.47		−0.07	0.81	1.91	1.14
sd^3	V^+	5.66	5.69	7.90	7.06	Nb^+	5.15	5.29	7.71	6.93
d^4		5.81	6.06	7.40	6.73		4.42	5.19	7.34	6.60
s^2d^4	Cr	0.00	0.00	0.00	0.00	Mo	0.00	0.00	0.00	0.00
sd^5		−1.27	−1.06	0.15	−1.00		−2.89	−2.37	−0.04	−1.47
d^6		5.76	6.07	2.04	3.40		1.03	1.99	0.94	1.71
sd^4	Cr^+	5.79	5.83	8.27	7.28	Mo^+	5.23	5.37	8.06	7.22
d^5		4.64	4.94	7.35	5.76		2.98	3.86	7.11	5.63
s^2d^5	Mn	0.00	0.00	0.00	0.00	Tc	0.00	0.00	0.00	0.00
sd^6		3.33	3.53	−0.31	2.14		0.20	0.75	−0.77	0.41
d^7		9.15	9.49	2.34	5.59		2.63	3.69	−0.31	—
sd^5	Mn^+	5.90	5.95	8.62	7.43	Tc^+	5.29	5.43	8.36	7.28
d^6		6.12	7.05	6.62	7.80		6.12	7.05	6.62	7.80
s^2d^6	Fe	0.00	0.00	0.00	0.00	Ru	0.00	0.00	0.00	0.00
sd^7		1.80	2.06	−0.74	0.87		−1.42	−0.74	−1.46	−0.87
d^8		7.46	7.87	0.71	4.07		0.27	1.50	−1.53	0.22
sd^6	Fe^+	6.28	6.34	8.95	7.90	Ru^-	5.68	5.87	8.65	7.59
d^7		7.95	8.33	7.00	8.15		4.50	5.57	6.14	6.50
s^2d^7	Co	0.00	0.00	0.00	0.00	Rh	0.00	0.00	0.00	0.00
sd^8		1.53	1.83	−1.13	0.42		−2.19	−1.40	−2.22	−1.63
d^9		7.04	7.53	0.11	3.36		−1.24	0.14	−2.85	−1.29
sd^7	Co^+	6.64	6.72	9.27	8.28	Rh^+	6.03	6.28	8.90	7.98
d^8		7.77	8.22	6.87	7.85		3.73	4.93	5.56	5.85
s^2d^8	Ni	0.00	0.00	0.00	0.00	Pd	0.00	0.00	0.00	0.00
sd^9		1.27	1.63	−1.51	−0.03		−3.01	−2.09	−2.97	−2.43
d^{10}		5.47	6.04	−0.46	1.71		−3.76	−2.19	−4.18	−3.38
sd^8	Ni^+	6.98	7.09	9.48	8.67	Pd^+	6.36	6.66	9.14	8.32
d^9		7.61	8.12	6.74	7.59		2.91	4.25	4.98	5.13
s^2d^9	Cu	0.00	0.00	0.00	0.00	Ag	0.00	0.00	0.00	0.00
sd^{10}		−0.37	0.06	−1.83	−1.49		−4.91	−3.86	−3.71	−3.97
sd^9	Cu^+	7.32	7.45	9.88	9.04	Ag^+	6.66	7.02	9.37	8.64
d^{10}		6.04	6.62	6.67	6.23		1.00	2.47	4.40	3.60

Table 2 *continued*

		NHF	HFR	PP	EXP			NHF	HFR	PP	EXP
s^2d	Lu	—	—	0.00	0.00	s^2d^5	Re	0.00	0.00	0.00	0.00
sd^2		—	—	2.76	2.37	sd^6		−0.04	1.76	1.37	1.76
d^3		—	—	5.68	—	d^7		2.05	5.80	3.36	—
sd	Lu^+	—	—	7.49	7.16	sd^5	Re^+	5.19	5.79	9.38	7.88
d^2		—	—	9.67	9.27	d^6		5.98	9.35	10.02	—
s^2d^2	Hf	0.00	0.00	0.00	0.00	s^2d^6	Os	0.00	0.00	0.00	0.00
sd^3		−0.38	0.95	1.33	1.69	sd^7		−1.63	0.55	0.79	0.75
d^4		1.72	4.37	4.96	—	d^8		−0.40	3.85	2.30	—
sd^2	Hf^+	5.07	5.61	8.08	7.17	sd^6	Os^+	5.58	6.40	9.75	8.77
d^3		5.12	7.54	9.80	9.12	d^7		4.37	8.17	9.75	—
s^2d^3	Ta	0.00	0.00	0.00	0.00	s^2d^7	Ir	0.00	0.00	0.00	0.00
sd^4		−1.28	0.21	1.82	1.04	sd^8		−2.43	0.09	0.20	0.40
d^5		−0.18	2.94	4.57	1.02	d^9		−2.08	2.63	1.23	2.90
sd^3	Ta^+	5.13	5.71	7.56	7.90	sd^7	Ir^+	5.94	6.97	10.09	9.05
d^4		4.51	7.28	9.71	9.37	d^8		3.55	7.74	9.44	—
s^2d^4	W	0.00	0.00	0.00	0.00	s^2d^8	Pt	0.00	0.00	0.00	0.00
sd^5		−2.95	−1.29	1.90	−0.18	sd^9		−3.28	−0.40	−0.43	−0.64
d^6		0.73	4.16	4.29	—	d^{10}		−4.69	0.50	0.05	−0.16
sd^4	W^+	5.17	5.77	8.97	7.94	sd^8	Pt^+	6.26	7.51	10.39	9.22
d^5		3.06	6.20	10.20	8.35	d^9		2.68	7.26	9.05	8.46
s^2d^9	Au	0.00	0.00	0.00	0.00						
sd^{10}		−5.13	−1.86	−1.08	−1.74						
sd^9	Au^+	6.56	8,03	10.68	9.76						
d^{10}		0.78	5.79	8.65	7.48						

An overall better agreement with experiment for our PP calculation than for HF or CG results can be seen from table 2. Calculated values of three ionisation potentials (IP) given in figure 3 also agree with experiment [39]. Analysis of table 2 and of figure 3(*a*) shows that the accuracy of the spectra of 3d atoms is worse than for heavier elements of the 4d and 5d rows. For example, the spin-unpolarised version of the LDA used here was not able to reproduce the relatively deep gaps in the IP versus Z_v curves. The electron correlation contribution seems to be overestimated in the LDA since we have usually obtained the 'd electron rich' configuration as being more stable than the 's electron rich' one for 3d elements, contrary to experimental data. This error is of smaller importance for 5d elements, where relativistic effects become rather too large to stabilise the 's electron rich' configurations in accordance with experiment (see table 2). In fact the IP versus Z_v curves for 5d elements are in better qualitative and quantitative agreement with experiment (see figure 3(*c*)), and all stable configurations for 5d atoms and ions are predicted correctly.

Quite recently IPs for 4d and 5d transition metals were recalculated [40] using the self-interaction-corrected LSD scheme in a quasirelativistic CG [38] approach. In most cases these results were in better agreement with experiment than either previous CG [37] or our own RLDA data, the maximum error reaching 0.5 eV. Nevertheless the overall improvement in the IP versus Z_v curves in comparison with our results (figure 3) was only of the order of 0.2–0.4 eV, and sometimes our data were in even better agreement with experiment. Thus we may conclude that, for 5d elements, spin-polarisation and

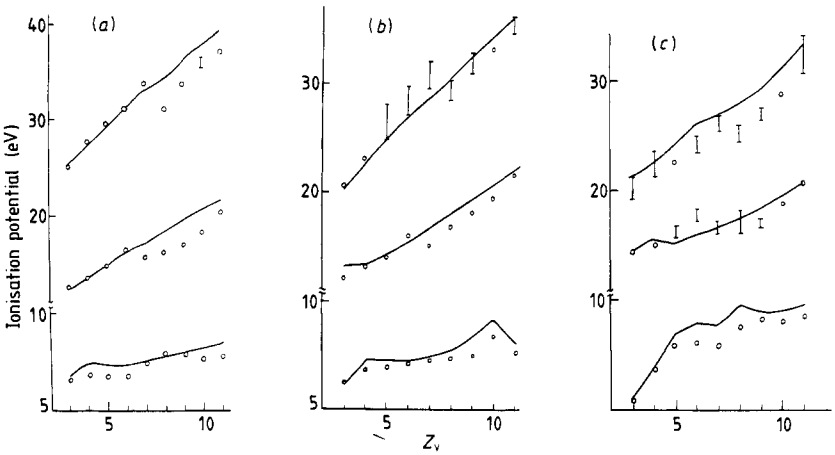

Figure 3. Three first-ionisation potentials for transition elements. Experimental data given by open circles and vertical bars are taken from [39]: (*a*) 3d elements from Sc to Cu; (*b*) 4d elements from Y to Ag; and (*c*) 5d elements from Lu to Au.

self-interaction effects are of minor importance compared with relativistic effects. As a whole the LDA provides good accuracy for atomic spectra, while for light 3d elements with unscreened d electrons spin-polarisation effects are probably more important than relativistic corrections.

4. Systematic trends in PPs for transition metals

In this section we intend to study some trends definitely manifested in the changes of PP characteristics along the rows of transition elements atoms. Some of them simply represent consequences of general trends observed in the Periodic table while others reflect merely the peculiarities of the PP treatment.

Among more general features we can note the obvious contraction of the valence shell resulting from its filling. This effect may be seen from figure 4 as the $r_{c\kappa}$-values represent scaled radii of the outermost peaks of the corresponding atomic valence wavefunction. This contraction is revealed also in a monotonic decrease of r_{min} corresponding to the position of $V_d^i(r)$ minimum. Note that r_{min} depends strongly on the number of d electrons in the 3d row, while for 5d elements it remains nearly unchanged due to the screening by inner d electrons.

The dependence of $r_{c\kappa}$ versus Z_v is not quite monotonic. A similar feature would be seen even better in the ε_κ versus Z_v curves where ε_κ represents the valence energies in reference atomic configurations. These 'serrated' dependencies, arising from irregular alternations of ground state configurations in the Periodic table, do not result in a similar dependence of PP parameters. For example, the Z_v dependence of the PP depth V_{min} is very smooth for all κ-components, an example for the d component is shown in figure 5. We would also notice some unusual features inherent in the PP obtained.

The PP acting on d electrons in 3d elements is very large and short-ranged, being weaker than the Coulomb potential only in the immediate vicinity of the nucleus. Its maximum depth is nearly five times larger than for 4d or 5d elements, and the corresponding radius r_{min} is nearly four times smaller. The very fast increase of V_{min} with

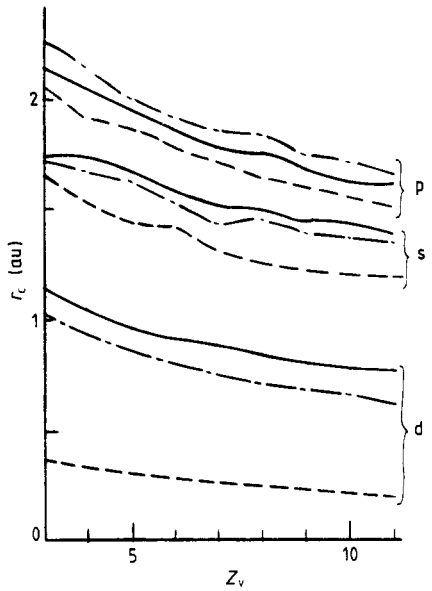

Figure 4. Cutoff radii r_{cK} for 3d (broken curve), 4d (chain curve) and 5d elements (full curve). Values are given for the $j = l + \frac{1}{2}$ component only.

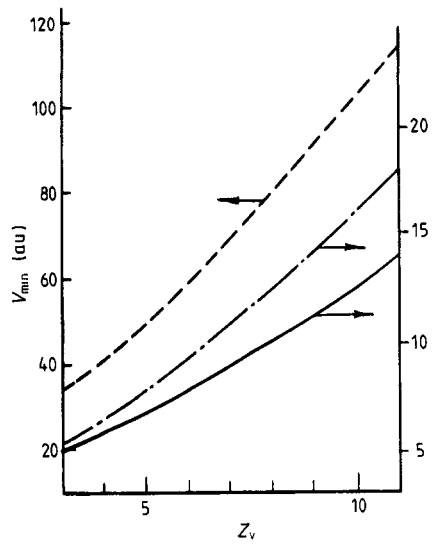

Figure 5. Depth of the $d_{3/2}$ PP potential for 3d (broken curve), 4d (chain curve) and 5d elements (full curve). Components with $j = l - \frac{1}{2}$ were used.

Z_v accompanied by an r_{min} decrease may be attributed to the resonance character of the interaction of the unscreened 3d electrons with the ionic core.

The dependence of V_{min} versus Z_v for s and p components is characterised by sufficiently smaller values of the PP in comparison with that of the d component. At the beginning of any transition row we have $V^s_{min} \simeq V^p_{min} \simeq 1$ au, and the smooth increase of V_{min} caused by d shell filling results in values of $V^s_{min} \simeq 10$ au and $V^p_{min} \simeq 5$ au at the end of the row. It is interesting that for 4d and for 5d elements, the s potentials are similar, and their $V^s_{min}(Z_v)$ and $r^s_{min}(Z_v)$ curves appear to be indistinguishable on the scale of e.g. figure 5.

Spin–orbit splitting in the PP was characterised by the value of ΔV_l determined as the maximum value of $V^i_{l-1}(r) - V^i_l(r)$. A plot of ΔV_l versus Z_v is given in figure 6. Previously the conclusion of maximum spin–orbit splitting for p states with a $\Delta V_p > \Delta V_d > \Delta V_f$ sequence was drawn [21]. Our results show that another relation $\Delta V_d > \Delta V_p > \Delta V_f$ is valid for all transition metals except for the first elements of the 3d and 4d series where $\Delta V_p \geqslant \Delta V_d$ is appropriate. The spin–orbit splitting ΔV_d smoothly increases with Z_v, while the ΔV_p versus Z_v curve presented in figure 6(*b*) is less smooth, and the ΔV_p increase is less pronounced. Note that the $\Delta V_p(Z_v)$ curve for 4d elements is close to that for 5d elements, so the former is not shown in figure 6(*b*).

The pseudopotential spin–orbit splitting has also been studied [41] for a number of simple metals using the relativistic quantum defect theory and the Heine–Abarenkov model PP. These values of ΔV_l were a few times smaller than those given in figure 6 due to a quite different form of PP components used in real space (V^i_K = const for $r \leqslant 2.5$ in [41]). Nevertheless, some trends in the $\Delta V_l(Z_v)$ dependence for simple metals resemble our results, e.g. the filling of the p shell leads to a decrease of ΔV_d with a simultaneous smooth increase of ΔV_p. It means that the $\Delta V_p > \Delta V_d$ relation obtained in [21, 41] for a variety of simple metals should be compared with $\Delta V_d > \Delta V_f$ for transition elements.

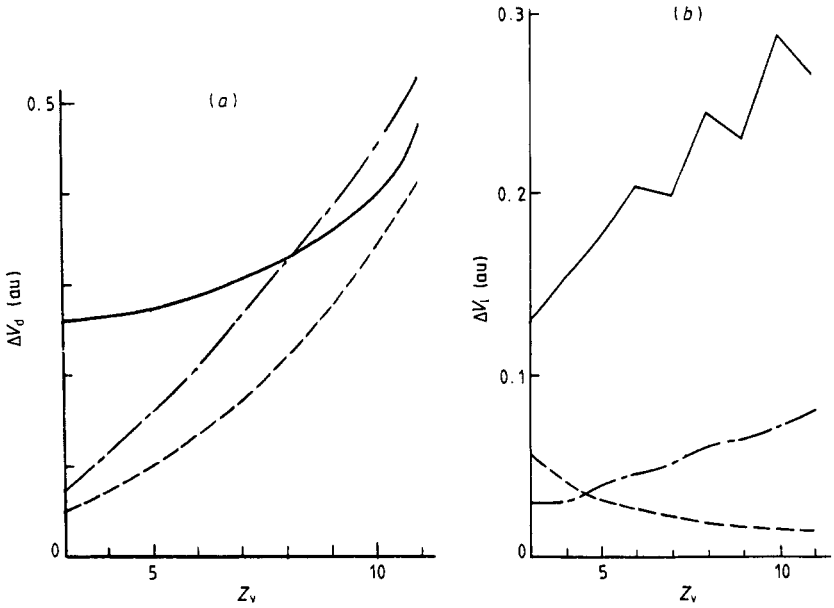

Figure 6. Spin–orbit splitting in the potential ΔV_l: (*a*) d component for 3d (broken curve), 4d (chain curve), and 5d elements (full curve); (*b*) p component for 5d (full curve) and 3d elements (chain curve), and the f component for 5d elements (broken curve).

Spin-orbit splitting increases for the valence states (d for transition elements and p for simple ones) and falls for the outer-core states (f for transition elements and d for simple) while going along a row of the Periodic table.

Now we make some comments on the technique of PP construction. First of all we studied the influence on V_κ^i of a particular choice of V_{xc} from [23, 35, 36] respectively, and found numerical differences in V_κ^i of the order of 1%. Then we performed pseudoatomic calculations for different configurations similar to those shown in table 1. At this stage we constructed $V(r)$ for the pseudoatomic problem (1.1) by choosing one of the three types of V_κ^i mentioned above, and $V_{xc}(p_{ps})$ was taken to be of the form given by Ceperley and Alder [23, 24]. The resulting valence energies were compared with each other and with all-electron data. All four sets of ε_κ and E_{ex} agree to within 0.1% thus confirming the negligible influence of the form of V_{xc} on the resulting V_κ^i.

Ionic PPs are considerably more affected by the choice of $r_{c\kappa}$-values. Reduction of $r_{c\kappa}$ by means of e.g. the choice of $K_l = 2$ for $l = 0, 1, 2$ leads, in the case of tungsten, to the emergence of the strong repulsive part of the PP at small distances. It should be noted that all components remain nearly unchanged in the small region of space near $r = 2$, i.e. in the region which determines a chemical bonding. The energy dependence of such a contracted potential is even weaker than the one illustrated by table 1. Thus one may choose the set of K_l-values according to the particular physical problem with confidence in transferability and accuracy of PP obtained.

5. Conclusions

In the present work, a formalism of ionic PP construction using a fully relativistic LDA treatment has been developed. PPs for transition metals of the third, fourth and fifth

rows were constructed, and systematic trends in the above series of elements were studied. Analysis of the major and minor wavefunction components indicates the necessity of a fully relativistic treatment of d electrons in heavy 5d elements.

Atomic energy eigenvalues and excitation energies are reproduced by our potentials with an accuracy of order 10 meV in the range of excitation energies up to 30 eV, which is evidence of good potential transferability. The resulting PPs are not sensitive to the particular form of the exchange–correlation potential. The short-range part of the potential is strongly influenced by the choice of effective ionic radii, leaving some flexibility for physical applications.

Acknowledgments

We are grateful to Professor V G Vaks and Dr N E Zein for numerous stimulating discussions. One of the authors (VNA) wishes to acknowledge extensive discussion of the concepts presented here with Professor V Heine and Professor O K Andersen. Another author (VYM) is grateful to Professor V Heine, Dr R W Godby and to their colleagues from the TCM Group in the Cavendish Laboratory, Cambridge, for their hospitality and significant help at the final stage of the work on this manuscript.

References

[1] Louie S G 1984 *Electronic Structure, Dynamics and Quantum Structural Properties of Condensed Matter* ed J T Devreese (New York: Plenum) pp 335–98
[2] Ho K-M, Fu C-L and Harmon B N 1983 *Phys. Rev.* B **28** 6687–94; 1984 *Phys. Rev.* B **29** 1575–87
[3] Lam P K, Dacorogna M M and Cohen M L 1986 *Phys. Rev.* B **34** 5065–9
[4] Dacorogna M M, Cohen M L and Lam P K 1986 *Phys. Rev.* B **34** 4865–7
[5] Rabe K and Joannopoulos J D 1987 *Phys. Rev. Lett.* **59** 570–3
[6] Ye Y Y, Chen Y, Ho K-M, Harmon B N and Lindgård P-A 1987 *Phys. Rev. Lett.* **58** 1769–72
[7] Zhu M J, Bylander D M and Kleinman L 1987 *Phys. Rev.* B **36** 3182–5
[8] Oshiyama A and Saito M 1987 *J. Phys. Soc. Japan* **56** 2104–12
Lee S, Bylander D M and Kleinman L 1989 *Phys. Rev.* B **40** 8399–403
[9] Zunger A and Cohen M L 1978 *Phys. Rev.* B **18** 5449–72; 1979 *Phys. Rev.* B **20** 4082–108
[10] Hamann D R, Schlüter M and Chiang C 1979 *Phys. Rev. Lett.* **43** 1494–7
[11] Kerker G P 1980 *J. Phys. C: Solid State Phys.* **13** L189–95
[12] Chulkov E V, Sklyadneva I Yu and Panin V E 1984 *Phys. Status Solidi* b **121** 265–74
[13] Lee Y S, Ermler W C and Pitzer K S 1977 *J. Chem. Phys.* **67** 5861–76
[14] Zunger A 1980 *Phys. Rev.* B **22** 5839–72
[15] Villars P 1986 *J. Less-Common Met.* **119** 175–88
[16] Zhang S B and Cohen M L 1989 *Phys. Rev.* B **39** 1077–80
[17] Lundqvist S and March N H (ed) 1983 *Theory of the Inhomogeneous Electron Gas* (New York: Plenum)
[18] Woodward C and Kunz A B 1988 *Phys. Rev.* B **37** 2674–7
[19] Ishikawa Y and Malli G 1981 *J. Chem. Phys.* **75** 5423–31
[20] Kleinman L 1980 *Phys. Rev.* B **21** 2630–1
[21] Bachelet G B, Hamann D R and Schlüter M 1982 *Phys. Rev.* B **26** 4199–228
[22] Greenside H S and Schlüter M 1983 *Phys. Rev.* B **28** 535–43
[23] Ceperley D M and Alder B J 1980 *Phys. Rev. Lett.* **45** 566–9
[24] Perdew J P and Zunger A 1981 *Phys. Rev.* B **23** 5048–79
[25] Hedin L and Lundqvist B I 1971 *J. Phys. C: Solid State Phys.* **4** 2064–83
[26] Ceperley D M 1978 *Phys. Rev.* B **18** 3126–38
[27] MacDonald A H and Vosko S H 1979 *J. Phys. C: Solid State Phys.* **12** 2977–90
[28] Kang M H, Tatar R C, Mele E J and Soven P 1987 *Phys. Rev.* B **35** 5457–72

[29] Zein N E 1984 *Sov. Phys.–Solid State* **26** 1825–8
Milman V Yu, Antonov V N and Nemoshkalenko V V 1988 *Fiz. Metall. Metalloved.* **66** 24–33 (in Russian)
[30] Kleinman L and Bylander D M 1982 *Phys. Rev. Lett.* **48** 1425–8
[31] Louie S G, Froyen S and Cohen M L 1982 *Phys. Rev.* B **26** 1738–42
[32] Bylander D M and Kleinman L 1983 *Phys. Rev.* B **27** 3152–9
[33] Bylander D M and Kleinman L 1984 *Phys. Rev.* B **29** 2274–6
[34] Vanderbilt D 1985 *Phys. Rev.* B **32** 8412–5
[35] Ihm J, Zunger A and Cohen M L 1979 *J. Phys. C: Solid State Phys.* **12** 4409–22
[36] Kohn W and Sham L J 1965 *Phys. Rev.* **140** A1133–8
[37] Martin R L and Hay P J 1981 *J. Chem. Phys.* **75** 4539–45
[38] Cowan R D and Griffin D C 1976 *J. Opt. Soc. Am.* **66** 1010–4
[39] Radzig A A and Smirnov B M 1986 *Parameters of Atoms and Atomic Ions* (Moscow: Energoatomizdat) (in Russian)
[40] Guo Y and Whitehead M A 1988 *Phys. Rev.* A **38** 3166–74
[41] Nandi M and Chatterjee S 1978 *Indian J. Phys.* A **52** 213–7
[42] Elsässer C, Takeuchi N, Ho K M, Chan C T, Brawn P and Fähnle M 1990 *J. Phys.: Condens. Matter* **2** 4371–94